Choroidal Neovascularization in the Yucatan Minipigs: A Laser-induced Model of Neovascular Age-related Macular Degeneration

Joshua T. Bartoe[1], Ryan F. Boyd[1], Krishna Yekkala[2], Alexander B. Quiambao[3], Didier J. Nuno[3], Rafal A. Farjo[3], and Thomas S. Vihtelic[1]

(1) Ophthalmology Services and (2) Anatomic Pathology, MPI Research, Mattawan, MI; (3) EyeCRO, Oklahoma City, OK

INTRODUCTION

Historically, large animal models of neovascular age-related macular degeneration have been unpredictable, with only 70% of laser-induced choroidal neovascularization (CNV) lesions in nonhuman primates (NHP) considered clinically relevant. Furthermore, only up to 40% of these CNV lesions are considered ideal, exhibiting Grade IV leakage on fluorescein angiography. This inefficiency leads to excess animal use and high study cost. Previous swine CNV models displayed extensive retinal damage and only minimal choroidal involvement when neovascularization was present.

OBJECTIVE

Our study aimed to create a reproducible, predictable swine model of laser-induced CNV, improving efficiency and lowering cost compared to available NHP CNV models.

METHODOLOGY

Fifteen Yucatan minipigs were used to optimize laser induction of CNV. Bilaterally, six lesions were created along the visual streak using a 532nm green argon laser under direct visualization with a slit lamp and condensing lens. After optimal laser settings were established, efficacy was assessed using bevacizumab as a positive control article. The first efficacy phase (N=3) involved unilateral intravitreal injection of 1.25mg bevacizumab, with the contralateral eye receiving balanced salt solution (BSS) on Day 3 following laser induction. In the second phase (N=4) either 1.25 mg bevacizumab or BSS was injected into both eyes on the day of laser induction. Follow-up examinations included optical coherence tomography (OCT) and fluorescein angiography (FA) at five-day intervals, followed by histopathology 10 days post-laser induction. Lesion relative intensity quantification was performed by multiple blinded observers on FA images using previously described methods. Briefly, each lesion was outlined by hand in Image J software to obtain mean lesion pixel intensity. A background intensity measurement was also taken from a vessel-free region adjacent to each lesion. Mean image background intensity was subtracted from each lesion mean intensity, the resulting value was divided by the maximum pixel intensity of the image to obtain a relative intensity value for the lesion. Mean relative intensity of all lesions for each eye was calculated; these values were compared between bevacizumab and BSS eyes using an unpaired Student's t-test.

RESULTS

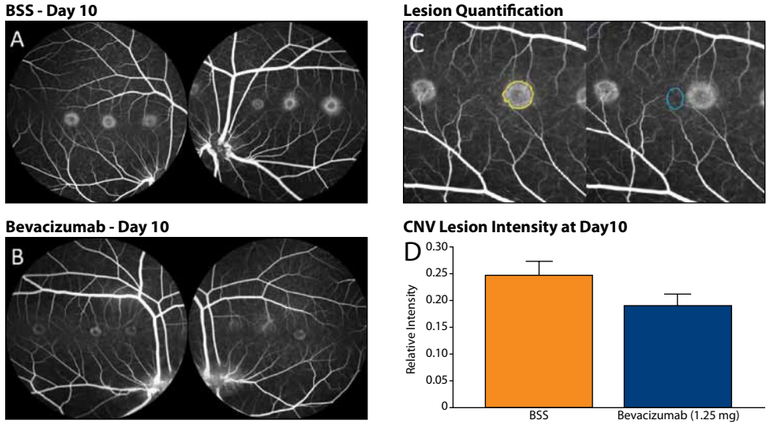

Figure 2: Quantification of relative lesion intensity. Fluorescein angiography images 10 days after laser induction and intravitreal injection of balanced salt solution (BSS, **A**) and 1.25 mg bevacizumab (**B**). Relative lesion intensity was calculated using Image J software to measure mean fluorescence within each lesion (**C**, yellow tracing), subtracting background intensity (**C**, blue oval), and dividing by the maximum pixel intensity within the image. Bar graph (**D**) representing relative intensity between eyes treated with either BSS or bevacizumab (mean +/- SE). Unpaired t-test showed a reduction in mean relative intensity in bevacizumab treated eyes, which approached statistical significance (P=0.056).

Optimized laser settings reliably produced rupture of Bruch's membrane, with focal regions of discontinuity of the hyperreflective line representing the retinal pigment epithelium/Bruch's membrane complex on OCT. OCT of these regions showed ingrowth of hyperreflective tissue into outer retinal layers, and hyperfluorescence on FA, suggestive of choroidal fibrovascular proliferation into the retina. Histopathological characterization supported the *in vivo* findings with moderate to marked subretinal fibrosis and neovascularization extending from choroid into outer retina. Inner retinal layers were generally well preserved over the site of laser delivery. Lesion relative intensity quantification from both efficacy phases revealed a lower mean relative intensity in bevacizumab-treated eyes (0.19 +/-0.06) compared to BSS-treated eyes (0.25 +/-0.07). Four of 30 eyes that received laser induction developed a subretinal fibrovascular proliferation that bridged two lesions, often noted between lesions made closer together than average. One animal treated with BSS bilaterally during the second efficacy phase did not develop the typical increase in relative lesion intensity between Days 5 and 10, despite apparent disruption of Bruch's membrane on OCT.

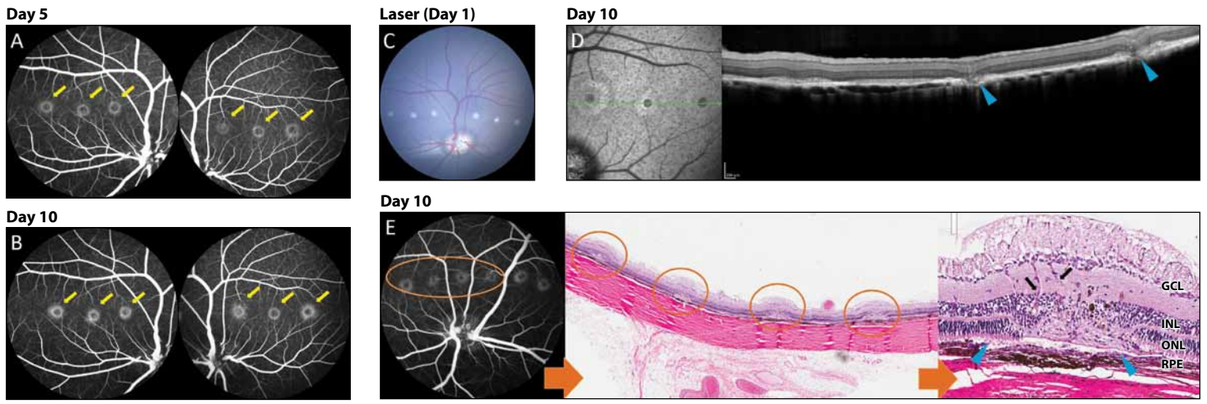

Figure 1: Lesion progression. Fluorescein angiography images 5 days (**A**) and 10 days (**B**) post-laser induction, demonstrating lesions made in a linear pattern along the visual streak (yellow arrows) and resultant fluorescein leakage at the site. A representative color funduscopic image taken immediately after laser induction is shown in panel **C**. Optical coherence tomography (**D**) and histopathology (**E**) both confirm discontinuity of RPE/Bruch's membrane at the site of laser delivery (blue arrowheads), with neovascularization extending into the preserved inner retinal layers (black arrows). GCL-ganglion cell layer, INL-inner nuclear layer, ONL-outer nuclear layer, RPE-Retinal pigmented epithelium

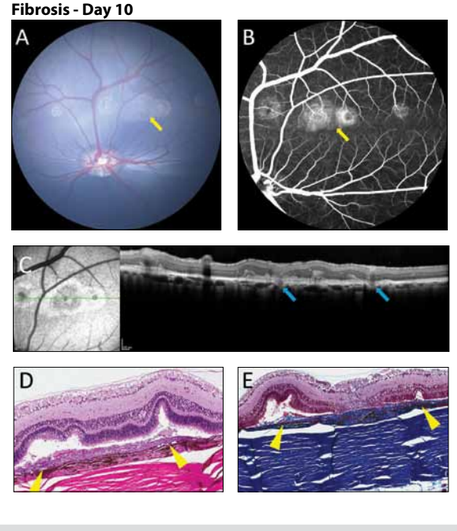

Figure 3: Subretinal fibrosis. A proliferative subretinal fibrovascular response extending between lesions was observed in 4/30 eyes. This was evident on both color fundoscopic imaging and fluorescein angiography (**A** and **B**, yellow arrows) as merging of two adjacent lesions. Optical coherence tomography revealed multifocal retinal elevation due to subretinal hyperreflective material extending between two Bruch's membrane defects (**C**, blue arrows). Marked subretinal fibroplasia with a mild subretinal hemorrhagic exudate is demonstrated by both hematoxylin and eosin and Masson's trichrome-stained sections (**D** and **E**, yellow arrowheads).

CONCLUSIONS

The Yucatan minipig is an excellent alternative to other large animal models of neovascular age-related macular degeneration. Similar globe size and retinal anatomy to human patients makes the swine model ideal for characterizing novel investigational molecules targeting proliferative posterior segment disease. The optimized laser settings generate a highly reproducible defect in Bruch's membrane while also minimizing damage to inner retinal layers, an important consideration for drug pharmacokinetics during pharmaceutical development. The response to laser injury is predictable in the swine model, with a lack of expected response in only one of the 13 animals not administered bilateral bevacizumab. The lesion quantification method used to calculate relative intensity for each lesion is an accurate objective measure of response to anti-VEGF compounds, with excellent inter-observer agreement (ICC=0.98). Linear placement of lesions permits high histopathology recovery rates using standard sectioning techniques. The proliferative fibrovascular response observed in some animals may be a valuable model for fibroplastic responses that accompany many posterior segment diseases. Additional effort is warranted to further characterize these lesions.

REFERENCES & ACKNOWLEDGEMENTS

1. Wang Q, et al. "Assessment of laser induction of Bruch's membrane disruption in monkey by spectral-domain optical coherence tomography." *Br J Ophthalmol.* 2015 Jan;99(1):119-24.
2. Criswell MH, et al. "The squirrel monkey: characterization of a new-world primate model of experimental choroidal neovascularization and comparison with the macaque." *Invest Ophthalmol Vis Sci.* 2004 Feb;45(2):625-34
3. Grossniklaus HE, Kang SJ, Berglin L. "Animal models of choroidal and retinal neovascularization." *Prog Retin Eye Res.* 2010 Nov;29(6):500-19
4. Goody RJ, et al. "Optimization of laser-induced choroidal neovascularization in African green monkeys." *Exp Eye Res.* 2011 Jun;92(6):464-72

The authors would like to acknowledge the contributions of Matthew Leahy, Stacy Patrick, and Benjamin Wilson for their technical support.

Disclosure Information: All Authors—None

Contact: josua.bartoe@mpiresearch.com